# TOMOGRAPHIC RECONSTRUCTION FROM PROJECTIONS WITH UNKNOWN VIEW ANGLES EXPLOITING MOMENT-BASED RELATIONSHIPS

*Eeshan Malhotra and Ajit Rajwade*

{eeshan, ajitvr}@cse.iitb.ac.in
Department of Computer Science and Engineering, IIT Bombay

## ABSTRACT

In this paper we describe a straightforward, yet effective method of recovering angles from a set of tomographic projections when the view-angles are completely unknown. Existing works on this problem have consistently assumed availability of projections from a large number of angles as well as made assumptions on the underlying distribution of angles to aid reconstruction. We make no such assumptions, and yet show a principled technique which is empirically seen to be quite robust to noise.

## 1. INTRODUCTION

Commonly, in a parallel-beam tomographic formulation, the view angles are assumed to be known. However, there are many scenarios where this may not be the case. One example scenario is cryo-electron microscopy (cryoEM), where tomographic techniques are used to determine the structure of a molecule or cell [1]. Multiple repetitions of the procedure are performed on identical specimens, which are arbitrarily oriented. With no way to control the relative orientation of the replica specimens, the tomographic angles are essentially unknown. Another use case of such a technique is in insect tomography [2], or tomography of objects performing unknown rigid motion, which is equivalent to performing a tomographic reconstruction on a fixed object, with the view angles of the projects being unknown. Uncertainty in view angles, though to a lower degree, may also occur due to patient motion in medical imaging [3].

In each of these scenarios, there may be significant or complete uncertainty in the angles from which tomographic projections are computed. It has been shown in [4] that under certain modest conditions, the view angles can be uniquely determined from the tomographic projections, and that the estimated angles are in principle stable under noise [5] in almost all cases. However the associated algorithms rely on some strong assumptions. Most algorithms make use of the assumption that projections at nearby angles are similar to each other, and utilize this assumption to formulate an embedding of projections onto a lower-dimensional space using dimensionality reduction techniques. [6] uses sLLE to embed projections on a circular, 2-D space; [7] utilizes spherical MDS to reduce dimensionality; [8] uses a Laplacian graph-based manifold learning method to embed projections from various view angles on the circle. Others such as [5] have utilized simple heuristics like a nearest neighbour search to find angle ordering. In all cases, the essence of the methodology has been to find out an *ordering* of angles. This suffers from multiple problems: First, since the assumptions are not mathematically driven, there is no theoretical guarantee on the resultant angles to satisfy the Helgasson-Ludwig Consistency conditions (See section 3.2), which relate the geometric moments of the underlying image to those of its tomographic projections. Second, since the algorithms provide only an ordering on the angles, one must depend on knowledge of the *underlying probability distribution* of the angles to recover the actual angle values. Lastly, the use of such methods necessitates the availability of projections from a large number of angles. Otherwise, the angle estimates have a large variance (Section III, [8]) In this paper, we describe a method which is mathematically motivated, general in applicability, robust to a fair degree of noise, and viable even with projections from a few angles being available.

## 2. BACKGROUND AND PROBLEM FORMULATION

In the problem of (parallel beam) tomographic reconstruction, the input consists of a set of angles, $\boldsymbol{\theta} \triangleq \{\theta_1, \theta_2, ..., \theta_P\}$ and the corresponding projections of a 2-D image from these angles, forming the set $\boldsymbol{P_\theta} \triangleq \{P_{\theta_i}\}_{i=1}^P$. A projection, $P_{\theta_i}$, is essentially a vector of line integrals of the image, as viewed from angle $\theta_i$ (from a fixed 0 angle). That is, the $s^{th}$ element of the vector $P_{\theta_i}$, $P_{\theta_i}(s)$, is the line integral along a ray at a distance $s$ from the origin, and inclined at an angle $\theta_i$ to the y-axis. It is well known that given infinitely many such projections with known corresponding angles, the image can be reconstructed perfectly. However this is infeasible in practice. Hence, multiple techniques have been developed to reconstruct images from a sparse set of projections, *e.g.*, the well-known filtered backprojection technique[9], or moment-based methods such as [10].

## 2.1. Unknown View Angles

In some applications, the exact angles in $\boldsymbol{\theta}$ are not known with precision, or not known at all. In such a situation, there is an inherent ambiguity associated with the angles being recovered. Rotating the initial image by a fixed angle $\phi$ would produce the exact same set of projections, but at an angular shift of $\phi$. Further, reflecting the original image also allows for the same set of projections to be produced. Therefore, all angles will be determined with this inherent ambiguity. That is, we may have an inherent ambiguity as $\hat{\theta}_i = \sigma\theta_i + 2n_i\pi + \phi$, where $\theta_i$ is the original angle from where the $i^{\text{th}}$ projection has been acquired, $\hat{\theta}_i$ is the estimated value of this angle, $\sigma \in \{+1, -1\}$, $n_i \in \mathbb{Z}$, and $\phi$ is the fixed rotational ambiguity. This is not a limitation as such, and we will evaluate the correctness of results allowing for such an ambiguity. It has been shown that provided a surprisingly small number of such projections, this problem permits a unique solution (allowing for aforementioned ambiguity) under very mild assumptions on the underlying image [4]. Further, the same authors have also proved that such a solution is stable under noise in [5]. However, a constructive algorithm to illustrate this, which does not rely on stronger assumptions on the distribution of the angles, has not been published. In the following section, we describe an algorithm that empirically satisfies these criteria.

# 3. ALGORITHM DESCRIPTION

The complete process consists of three basic parts: (1) Denoising noisy tomographic projections, (2) Angle estimation through coordinate descent, and (3) Image reconstruction using the estimated angles. In this work we provide algorithms for steps 1 and 2. Existing algorithms for step 3 perform quite well. For assessing the technique, we use the error in estimation of angles as a metric for evaluation. For testing, we have used filtered back-projection (FBP) algorithm for reconstruction, for simplicity, though better algorithms inspired from the compressed sensing literature may be used [11].

## 3.1. Denoising

We used a patch-based PCA denoising method to reduce the noise in the projections. This algorithm is adapted from the adaptive PCA denoising algorithm for 2-D images, as described in [12]. We consider patches of size $d \times 1$ from a moving window across each projection. For each patch, we find its $L$ nearest patches (in the $L^2$-norm sense). We perform PCA on this set of $L$ vectors and project each one along the principal directions to produce eigencoefficients. To denoise the patch, we manipulate these coefficients using Wiener-like updates of the form $\hat{x_{il}} = y_{il}\left(\dfrac{\sigma_l^2}{\sigma_l^2 + \sigma^2}\right)$, where $\hat{x_{il}}$ is an estimate of the $l^{\text{th}}$ denoised coefficient for patch $i$ ($1 \leq l \leq d$),

$y_{il}$ is the corresponding noisy coefficient for patch $i$, and $\sigma_l^2$ (the mean squared value of the $l^{\text{th}}$ coefficient across all $L$ patches) is estimated as: $\hat{\sigma}_l^2 = \max\left(0, \frac{1}{L}\sum\limits_{i=1}^{L} y_i^2 - \sigma^2\right)$.

Note that this is different from a PCA-based denoising approach as used in [13], where entire projections are compared. The patch-based approach proposed above has two distinct advantages: (1) The use of patches (with size appropriately tuned) allows for similarity among different parts of the same projection as well; and (2) This method works even when the total number of projections is considerably lower. When finding similarity between entire projections, in a small set, it is unlikely that we find very similar projections.

## 3.2. Coordinate Descent

This is the key part of the algorithm. We utilize the Helgasson-Ludwig Consistency Conditions (HLCC) [14], which describe the relationship between the geometric moments of the underlying image $f(x, y)$ and its projections from a given angle. For a particular angle $\theta_i$, the $n^{\text{th}}$ order moment of $P_{\theta_i}$ is calculated as follows:

$$m_{\theta_i}^{(n)} = \int_{-\infty}^{\infty} P_{\theta_i}(s)s^n ds \tag{1}$$

Now, there exist $n + 1$ image moments of the $n^{\text{th}}$ order. For natural numbers $p, q$, such that $p + q = n$, the $n^{\text{th}}$ order image moments can be calculated as [9]:

$$v_{p,q} = \int_{-\infty}^{\infty} \int_{-\infty}^{\infty} f(x, y)x^p y^q dx dy \tag{2}$$

The HLCC describe a relationship between the $n^{th}$ order projection moments and the $n^{\text{th}}$ order image moments:

$$m_{\theta_i}^{(n)} = \sum_{j=0}^{n} \binom{n}{j}(\cos\theta_i)^{n-j}(\sin\theta_i)^j v_{n-j,j} \tag{3}$$

Using projection moments from multiple angles, equation 3 can be written in matrix form, $\mathbf{m}^{(\mathbf{n})} = \mathbf{A}^{(\mathbf{n})}\boldsymbol{v}^{(\boldsymbol{n})}$ where, for the $n^{th}$ order equation, $\mathbf{A}^{(\mathbf{n})}$ is the $P \times (n + 1)$ matrix defined by $\mathbf{A}^{(\mathbf{n})}{}_{ij} = \binom{n}{j}(\cos\theta_i)^{n-j}(\sin\theta_i)^j$, and $\boldsymbol{v}^{(\boldsymbol{n})} \triangleq \{v_{p,q}|p + q = n, p, q \in \mathbb{Z}\}$, and $\mathbf{m}^{(\mathbf{n})}$ is a vector containing the projection moments of order $n$ at $P$ different angles. This equation can be used to determine $\boldsymbol{v}^{(\boldsymbol{n})}$, and for this, we need $P \geq n + 1$.

Since, in practice, the projections are noisy, despite denoising, equation 3 will not be satisfied exactly. Further, uncertainty in the value of $\theta_i$s will translate into more approximation errors. In our problem setting, we do not actually know the values of $\theta_i$. We will, instead, use *hypothesized* values of $\theta_i$. For hypothesized values of $\boldsymbol{\theta}$ and the set of image

moments, $\boldsymbol{v} = \{\boldsymbol{v}^{(n)}\}_{n=0}^k$, we can define our energy function, $E$ as:

$$E(\boldsymbol{\theta}, \boldsymbol{v}) = \sum_{n=0}^{k} \sum_{i=1}^{p} \left( m_{\theta_i}^{(n)} - \sum_{j=0}^{n} \mathbf{A}^{(\mathbf{n})}{}_{i,j} v_{n-j,j} \right)^2 \quad (4)$$

Equation 4 is the crux of the algorithm. $E(\boldsymbol{\theta}, \boldsymbol{v})$ is the objective we must minimize by appropriately selecting values of the parameters $\boldsymbol{\theta}$ and $\boldsymbol{v}$. This is achieved through an iterative approach, where estimates for each $\theta_i$ are improved one at a time, and the values of $\boldsymbol{v}$ recalculated using a pseudo-inverse. We can now describe the iterative algorithm using coordinate descent.

1: Randomly initialize $\boldsymbol{\theta}$ estimates, by picking each $\theta_i$ uniformly from $-\pi$ to $\pi$
2: Calculate projection moments, $m_{\theta_i}^{(j)}$, of the first $1 \leq j \leq k$ orders.
3: Estimate image moments of the first $k$ orders, $\boldsymbol{v}^{(i)}$, $1 \leq i \leq k$. We only need $k+1$ view angles for this, but we set $k$ to a much lower value than the number of available views, to introduce redundancy into the system.
4: Calculate $E$ using equation 4.
5: Set $\Delta E = \infty$
6: **while** $\Delta E > \epsilon$ **do**
7:     **for** each $\theta_i$ **do**
8:         **for** each angle in $-\pi$ to $\pi$, with appropriate resolution **do**
9:             Assume this value for $\theta_i$
10:             Recalculate image moments using this value
11:             Calculate $E$ again, using updated values of $\theta_i$ and image moments
12:             **if** $E$ calculated is lower than that using the previous best estimate for $\theta_i$ **then**
13:                 update the best estimate for $\theta_i$
14:                 $\Delta E = $ Old value of $E$ − new value of $E$
15:                 Update the value of $E$
16:             **end if**
17:         **end for**
18:     **end for**
19: **end while**

For each $\theta_i$, the algorithm performs a 1-D brute-force search for the value that minimizes $E$. The image moments are then re-estimated, and the value of $E$ updated At each step, exactly one $\theta_i$ is updated. Since each update always reduces $E$, and $E$ is a non-negative quantity, it is guaranteed to converge eventually. In practice, it is seen that it takes a small number of iterations to converge. Further, the highest order moment to consider, $k$ is a tunable parameter. When we increase $k$ by 1, we increase the number of knowns by $p$ - one known projection moment of order $k$ for each of the $p$ angles - and the unknowns by only $k$ - image moments of the $k^{\text{th}}$ order, introducing more redundancy in the system. So, in theory, it is feasible to use a very large $k$. However, in experiments, it was seen that while angle recovery generally improves with

increasing the value of $k$, going beyond order 6 or 7, the gain was not noticeable, but increased computation time significantly.

The search space is not convex, and so, the convergence point using coordinate descent may be sensitive to initialization values of $\theta_i$s. To counteract this to a certain extent, we used a multi-start strategy, where the above algorithm is run multiple times, each time with a random initialization for $\boldsymbol{\theta}$. Finally, the iteration with the least value of $E$ at convergence is chosen as the optimal set of assignments for $\boldsymbol{\theta}$. Using this multi-start strategy, we almost always obtained close to accurate angle estimates.

## 4. EXPERIMENTAL RESULTS

Experiments were conducted for multiple images, under zero mean, i.i.d. Gaussian noise with standard deviation varying from 1% to 10% of the standard deviation of the tomographic projections. It was observed that the final angles recovered were consistently close (within $\pm 5°$) to the actual angles used to compute the projections. To test the robustness of the algorithm to different angle distributions, experiments were conducted on angles sampled from (1) a $(0, 180)$ uniform distribution, (2) a non-uniform distribution, picking angles from each successive $30°$ interval in the ratio 0.2:0.3:0.12:0.3:0.35 and (3) an extremely peaky distribution with 10 angle values sampled close to each of 10 randomly chosen, spread out peaks. We emphasize that knowledge of this distribution of the angles was *not* used anywhere in our estimation algorithm.

Reconstruction results using filtered back-projection and with a set of 30 angles as input for a particular image are included in Figure 2 along with the angle estimation results in the top row of Figure 3. Although, reconstructed images are also shown for visual interpretation, it should be noted that the reconstruction suffers from significant noise because of the limitations of FBP, and should be considered only in comparison to the baseline provided alongside. While the reconstruction quality seems to have gone down when using a peaky distribution, it is a limitation of the FBP algorithm that causes this, and in fact, the quality of angle recovery can be seen in Figure 3 for different images and angle distributions at a noise level of 10%.

We compared our results to the algorithm in [13] which in turn builds upon prior work in [8] using the code provided by the authors. These methods are representative of the class of methods that assume knowledge of the angle distribution. While the method in [13] is indeed highly effective when the input consists of a large number of angles from a uniform distribution even at incredibly low SNRs, we observed in our experiments that it fails complete (error greater than $30°$) if either the number of angles is small (*e.g.*, 30 as in the experiment here), or if the distribution is not uniform. The former fact follows immediately from the formula for the variance of the angle estimates as provided in [8], section (III).
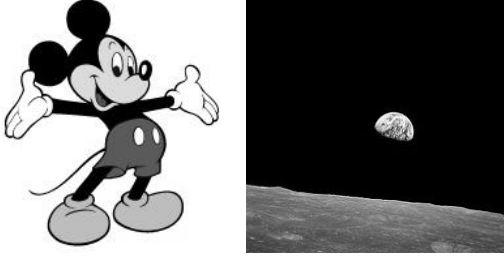
**Fig. 1**. Original images used. Reconstruction results in Fig 2
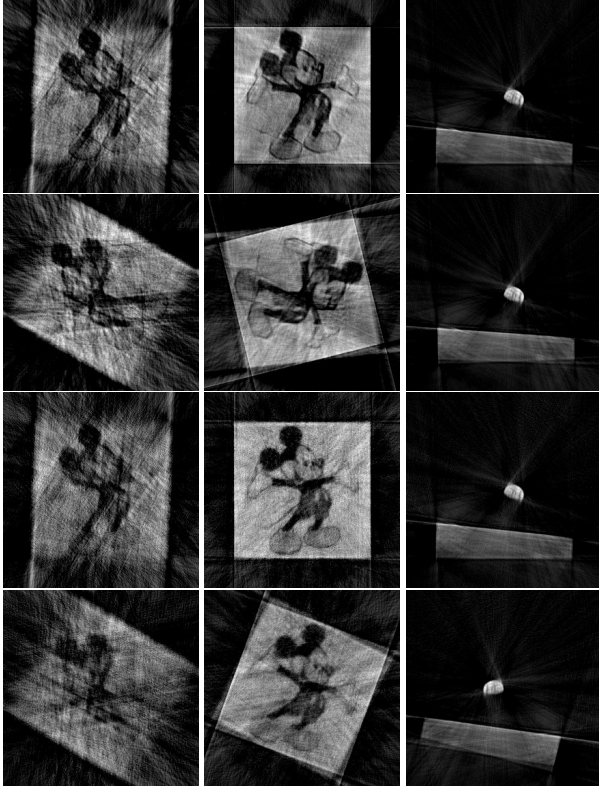


**Fig. 2**. FBP reconstruction using a non-uniform distribution of angles. Top to bottom: Using (1) 5% noise & actual angles, (2) 5% noise & estimated angles, (3) 10% noise & actual angles (4) 10% noise & estimated angles Reconstructions done with 30 angles (first column), 100 angles (second column), 100 angles (third column). Image canvas sizes have been expanded to allow for images to fit even when reconstructions are rotated.

## 5. SUMMARY AND CONCLUSIONS

We proposed a general method for image reconstruction from projections from unknown views and empirically demonstrated its efficiency in a wide variety of scenarios - With varying number of view angles, with different distributions for generation of the view angles, and at multiple noise levels. In particular, we focused on accurate recovery of angles from
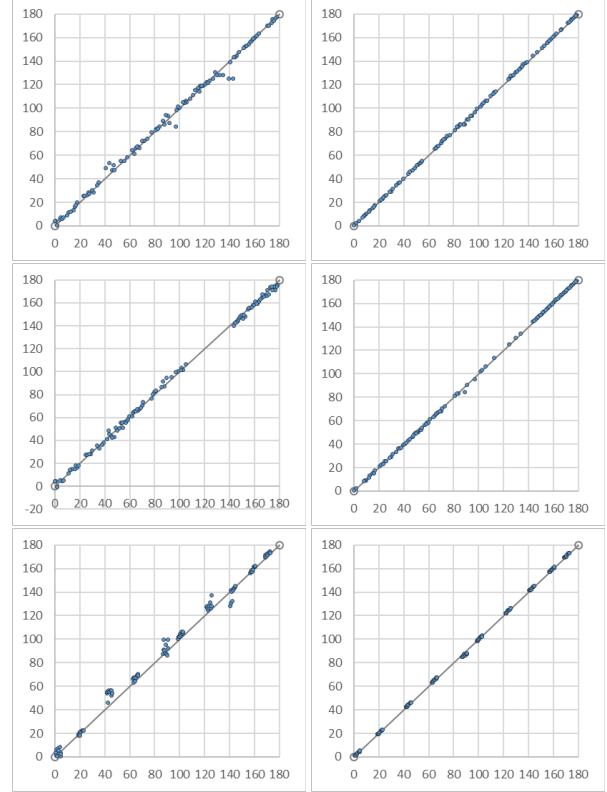


**Fig. 3**. In each figure, X and Y axes show true and estimated angles respectively, under 10% noise. Left: image 'mickey'; Right: image 'earthrise'. Angles drawn from - Top row: a uniform distribution; Middle: a non-uniform distribution; Bottom: very peaky distribution. For visualization, the offset $\phi$ in the estimated angles has been removed manually

which noisy projections are provided. The key idea was to iteratively improve angle estimates in order to reduce residuals in HLCC, using a coordinate descent strategy.

We experimented using multiple values of the maximum order of image moments in consideration. There is a clear trade-off between accuracy and computational time, but only up to a (fairly low) threshold, after which, barely any improvement was noticed in the recovered angles. However, this remains a parameter which must be tuned by the user. In practical applications, besides unknown view angles, different projections could be acquired at different and unknown shifts. This scenario can be handled easily assuming the background intensity as 0, since that would produce projections padded with an appropriate number of zeros (modulo noise).

There exist several open avenues for future research, such as handling projections with impulse noise or missing bins, projections with fan-beam geometry, reconstructions of 3D objects, and exploring the relationship of this problem with tasks such as automated instrument calibration in compressed sensing.

# 6. REFERENCES

[1] J. Frank, *Three-Dimensional Electron Microscopy of Macromolecular Assemblies*, Elsevier, 1996.

[2] S. Walker et al, "In vivo time- resolved microtomography reveals the mechanics of the blowfly flight motor," *PLOS BIOLOGY*, vol. 12, 2014.

[3] M. Wood, M. Shivji, and P. Stanchev, "Planar-motion correction with use of k-space data acquired in fourier MR imaging," *Journal of Magnetic Resonance Imaging*, vol. 5, no. 1, pp. 57–64, 1995.

[4] S. Basu and Y. Bresler, "Uniqueness of tomography with unknown view angles," *IEEE Transactions on Image Processing*, vol. 9, no. 6, pp. 1094–1106, 2000.

[5] S. Basu and Y. Bresler, "Feasibility of tomography with unknown view angles," *IEEE Transactions on Image Processing*, vol. 9, no. 6, pp. 1107–1122, 2000.

[6] Y. Fang, M. Sun, S. Vishwanathan, and K. Ramani, "sLLE: Spherical locally linear embedding with applications to tomography," in *Computer Vision and Pattern Recognition (CVPR), 2011 IEEE Conference on*. IEEE, 2011, pp. 1129–1136.

[7] Y. Fang, S. Murugappan, and K. Ramani, "Estimating view parameters from random projections for tomography using spherical mds," *BMC medical imaging*, vol. 10, no. 1, pp. 12, 2010.

[8] R. Coifman, Y. Shkolnisky, F. Sigworth, and A. Singer, "Graph laplacian tomography from unknown random projections," *IEEE Transactions on Image Processing*, vol. 17, no. 10, pp. 1891–1899, 2008.

[9] A. Rosenfeld and A. Kak, *Digital picture processing*, vol. 1, Elsevier, 2014.

[10] T. J. Wang and T. W. Sze, "The image moment method for the limited range CT image reconstruction and pattern recognition," *Pattern Recognition*, vol. 34, no. 11, pp. 2145–2154, 2001.

[11] S.J. Kim, K. Koh, M. Lustig, S. Boyd, and D. Gorinevsky, "An Interior-Point Method for Large-Scale l1-Regularized Least Squares," *Selected Topics in Signal Processing, IEEE Journal of*, vol. 1, no. 4, pp. 606–617, 2008.

[12] D. D. Muresan and T. Parks, "Adaptive principal components and image denoising," in *ICIP (1)*, 2003, pp. 101–104.

[13] A. Singer and H-T. Wu, "Two-dimensional tomography from noisy projections taken at unknown random directions," *SIAM journal on imaging sciences*, vol. 6, no. 1, pp. 136, 2013.

[14] F. Natterer, *The Mathematics of Computerized Tomography*, Wiley, 1986.